



Synthesis and Catalytic Activity of Nano Hydrotalcite with different Cations (Zn, Ni, Cu) for Transesterification of Vegetable Oil

Karthikeyan Chelladurai* and Manivannan Rajamanickam

**Department of Chemistry, Government Arts College (Autonomous)
Kumbakonam-612001, Tamilnadu, India**

Abstract: Biodiesel produced by the transesterification of vegetable oils is a promising alternative fuel to diesel because of limited fossil fuel resources and environmental concerns. The purpose of the present work was to synthesize and characterize Zn-Mg-Al, Ni-Mg-Al and Cu-Mg-Al Nano Hydrotalcites and performance of catalyst were evaluated by transesterification of vegetable oil like Ilupa oil (*Madhuca longifolia*) to Fatty acid methyl ester (FAME). A series of Zn-Mg-Al, Ni-Mg-Al and Cu-Mg-Al Nano Hydrotalcite samples have been synthesized by conventional co-precipitation method and calcined at 773-823K. The optimum reaction conditions were found to be at temperature 65°C, reaction time 4 hours, catalyst loading 7.5 g and methanol to oil molar ratio was 10:1. The catalysts were characterized by XRD, FT-IR, SEM, BET surface area analysis and biodiesel composition was confirmed by GC-MS techniques.

Keywords: Nano hydrotalcite, Layered double hydroxide, transesterification, biodiesel.

Introduction

Biodiesel is a biodegradable, renewable fuel, and essentially free of sulphur and aromatics makes it a cleaner burning fuel than petroleum diesel with reduced emissions of SO_x, CO, unburnt hydrocarbons and particulate matter¹⁻³. Biodiesel is a non-toxic and suitable replacement for fossil fuels. It is produced from nontoxic, biodegradable, renewable resources, such as new and used cooking oil and animal fats. Fats and oils chemically react with alcohols (transesterification reaction) to produce fatty acid methyl esters (biodiesel) and glycerin as a byproduct. Transesterification reaction is carried out in the presence of homogeneous or heterogeneous, acid or base catalysts.

In particular, Hydrotalcite (HT) has attracted interest as catalysts for transesterification of vegetable oil. Hydrotalcite also called layered double hydroxides (LDH). LDH is solids with interesting basic properties that show them to be efficient catalysts for transesterification reaction⁴. The LDH can be decomposed to mixed oxides with H₂O and CO₂ losses by Calcination. The mixed oxides formed are of particular interest due to their increased basicity relative to the LDH precursor, increased surface area, and homogeneous mixing of the different elements⁵. The most common method applied for preparation of hydrotalcite is co-precipitation, wherein precipitating agents such as NaOH or/and NaHCO₃ are added to the solution of metal salts⁵. LDH possesses a unique layered structure. On the other hand, during calcination at high temperatures the layered structure could easily be destroyed. The generally activation of HT involves a heat treatment wherein the layered structure is destroyed to form a mixed oxide. In a next step the material is rehydrated to restore the original HT structure to a large extent and with the exclusion of other anions and CO₂, Bronsted base sites (OH₂) are incorporated in the interlayer⁶⁻¹⁰.

We have already reported Mg-Al Nano catalysts with neem oil (*Azadirachta indica*) that gave a maximum ester conversion of 84% for the sample with 3:1 molar ratio¹¹ and Zn-Mg-Al Nano catalysts with neem oil (*Azadirachta indica*) gave maximum ester conversion of 90.5%¹². In this present work, dealt with the synthesis and characterization of Ni-Mg-Al, Zn-Mg-Al and Cu-Mg-Al Nano hydrotalcite and performance of hydrotalcite is analyzed by transesterification of Ilupa oil (*Madhuca longifolia*).

Materials and Methods

Ilupa oil (*Madhuca longifolia*) was purchased from the commercial market, chemicals such as $\text{Zn}(\text{NO}_3)_2 \cdot 6\text{H}_2\text{O}$, $\text{Mg}(\text{NO}_3)_2 \cdot 6\text{H}_2\text{O}$, $\text{Ni}(\text{NO}_3)_2 \cdot 6\text{H}_2\text{O}$, $\text{Cu}(\text{NO}_3)_2 \cdot 6\text{H}_2\text{O}$ and $\text{Al}(\text{NO}_3)_3 \cdot 9\text{H}_2\text{O}$ were purchased from Merck, and methanol, NaOH, and Na_2CO_3 were purchased from Sigma Aldrich. All chemicals used were of analytical reagent grade.

Catalysts Preparation

All the Nano hydrotalcites are synthesized by co-precipitation method. Solution A contains various molar ratios of $\text{Zn}(\text{NO}_3)_2 \cdot 6\text{H}_2\text{O}$, $\text{Mg}(\text{NO}_3)_2 \cdot 6\text{H}_2\text{O}$, and $\text{Al}(\text{NO}_3)_3 \cdot 9\text{H}_2\text{O}$ and solution B contains 2M NaOH and 0.125M Na_2CO_3 . Solution B is added to solution A under vigorous stirring at 338 K for 48 h, maintaining the pH between 8 and 10. The resulting precipitate was filtered and washed with water to eliminate the alkali metal ions and the nitrate ions and catalysts were dried at 383 K overnight. The samples were then calcined at 773-823 K in a muffle furnace for overnight. Ni-Mg-Al and Cu-Mg-Al Nano hydrotalcite also synthesized by this procedure. Catalysts with various molar ratios have been synthesized like 2:2:1, 2:3:1, 3: 3:1, and 3:5:1.

Catalysts Characterization

The crystalline characteristic was determined by using the X-ray diffraction instrument Siemens D-diffractometer using $\text{CuK}\alpha$ radiation ($\lambda = 1.5406 \text{ \AA}$). Scans were performed over the 2θ range from 10° to 70° . The particle size of the hydrotalcite was calculated using the Scherer equation. An FEI QUANTA200 Fourier transform infrared (FT-IR) spectrum was recorded on a Nicolet 5DX spectrophotometer using KBr pellet technique. Gas chromatography analysis was performed on a GC-2010 (Shimadzu, Japan). The chemical composition of the synthesized samples was determined using JEOL JCXA 733 EPMA (Electron Probe Microanalysis). Scanning electron Microscopy (SEM) measurements were carried out with a field emission microscope (JEOL, JSM-6400) equipped with an energy dispersive X-ray (EDX) analyzer, operated at an acceleration voltage of 40 kV. The specific surface area was measured by the flow method using Micromeritics Pulse Chemisorb 2700 instruments.

Catalytic Activity

The catalytic activity was evaluated using the transesterification of crude Ilupa oil (*Madhuca longifolia*) with methanol. Transesterification experiments were carried out in a four necked flask. A specified amount of mixed metal oxide catalyst and the required volume of methanol was added to the reaction mixture to Ilupa oil (*Madhuca longifolia*). The reactant mixture was then heated under maximum agitation. At the end of the experiment, the catalyst was separated from the product using a centrifuge, and the reaction mixture was then loaded into a rotary evaporator to remove excess methanol. The top layer was the biodiesel phase of the methyl esters and lower phase was glycerin. The chemical analysis was carried out by the gas chromatography.

Result and Discussion

X-Ray diffraction analysis

The XRD pattern of Zn-Mg-Al, Ni-Mg-Al and Cu-Mg-Al Nano Hydrotalcite represented in figure 1, 2 and 3 respectively. All Hydrotalcite shows strong, sharp, and symmetric peaks for the (003), (006), (110), and (113) planes as well as broad and asymmetric peaks for the (012) (015) and (018) planes, which is the characteristic of well-crystallized hydrotalcite.

In Zn-Mg-Al Nano hydrotalcite diffraction lines which could be attributed to the overlapping MgO and/or ZnO ^{13,14}. Figure 1 reveals peak at 11.46, 23.28, 33.57, 39.7, 47.1 and 60.9⁰ are characteristics of a layered structure¹² (JCPDS 54-1030). The peaks of Al_2O_3 phase were very small, indicating that Al^{3+} cations were

dispersed in the structure of MgO without the formation of spinel species¹⁵. The difference in the intensities of the reflections from one sample to another indicates different degrees of crystallinity when the cationic composition varies. The cationic ratio in the synthesized hydrotalcites was in good agreement with the theoretical one, as the electron micro probe analyzer (EPMA) results showed no major changing in the final composition. The unit cell parameters were done by the peaks indexing in the hexagonal crystal system which was presented in table 1. The values obtained here are close to previously reported data for similar materials^{16,17}. It can be noticed that the value “*a*” is not influenced by the nature of divalent cations incorporated in the brucite-like layers and do not lead to distortions in the octahedral planes¹⁸. The *a* and *c* parameters decreased with increasing aluminum content, which can be explained by the substitution of larger Mg²⁺ ions by smaller Al³⁺ ions¹⁶. It also indicates that the incorporation of Zn leads to an increase in stress in the octahedral hydroxide layer in the hydrotalcite crystal structure, due to the difference in ionic radii between Mg²⁺ and Zn²⁺ as there are no differences in the bond lengths around a single octahedral site. The average particle size was calculated as 20 nm by the Scherer equation [$D_c = k (\lambda/\beta) \cdot (\cos\theta)$] where *D_c* is the average particle size, *k* is the Scherer constant (0.89), λ is the X-ray wavelength, (CuK α) = 0.1541 nm, β is the FWHM (full-width at halfmaximum), and θ is the diffraction angle in the XRD (003) reflection¹⁹.

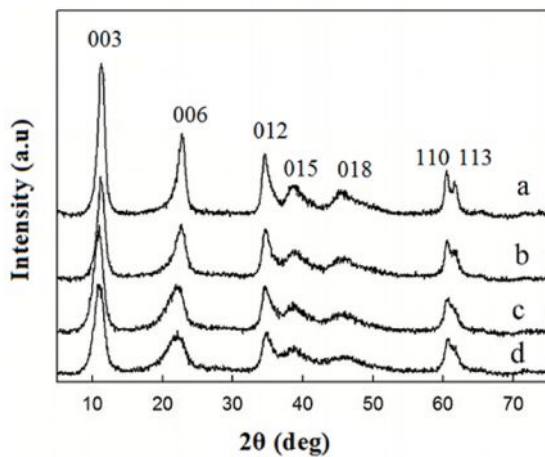


Figure 1: XRD pattern of (a). 2:2:1 (b). 2:3:1 (c). 3:3:1 (d). 3:5:1 molar ratio of Zn-Mg-Al Nano Hydrotalcite

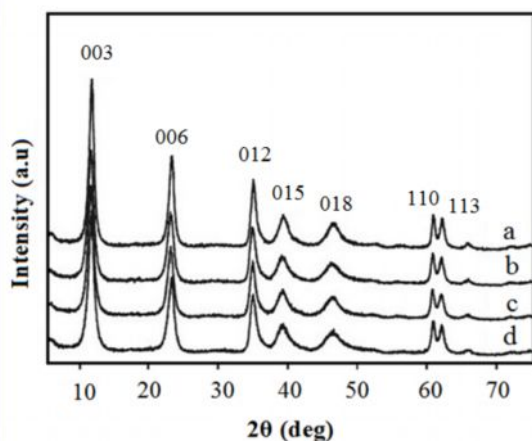


Figure 2: XRD pattern of (a). 2:2:1 (b). 2:3:1 (c). 3:3:1 (d). 3:5:1 molar ratio of Ni-Mg-Al Nano Hydrotalcite

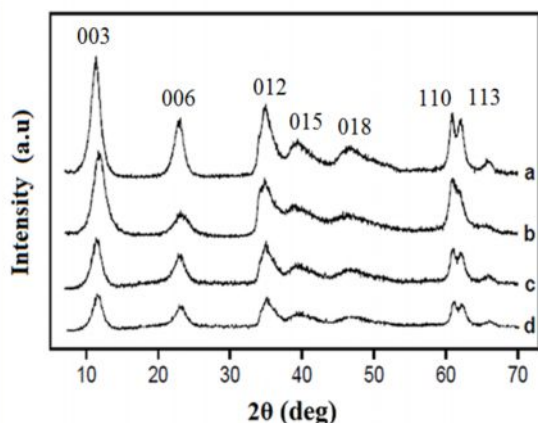


Figure 3: XRD pattern of (a). 2:2:1 (b). 2:3:1 (c). 3:3:1 (d). 3:5:1 molar ratio of Cu-Mg-Al Nano Hydrotalcite

The XRD patterns of Ni-Mg-Al catalyst were given in figure 2. It shows a peak at 11.5, 24.5, 34.0, 38.6, 45.8 and 60.8° which are characteristic of layered structure²⁰ (JCPDS 35-0965). The absence of other phases suggests that both Ni²⁺ and Al³⁺ have isomorphically replaced Mg²⁺ cations in the brucite-like layers. In this case, the XRD data indicate that both NiO and AlO are incorporated into the MgO matrix with no significant segregation of other crystal species apparent. This high dispersion of Ni and Mg/Al is desirable for higher catalytic activity²¹. For samples containing both Mg and Ni and Al, the oxides are mainly of the spinel phase with the characteristic diffraction peaks of NiAl₂O₄, Mg₂NiO₄ and magnesium aluminate, MgAl₂O₄ in addition to the individual spinel nickel oxides, and magnesium oxides MgO. The situation of overlapping is also observed between MgO and some of the spinels. The average particle size was calculated as 20 nm by the Scherer equation. The chemical compositions of Ni-Mg-Al are summarized in table 2. The elemental analysis and XRD results clearly correspond and show that the mixed oxides are homogenous and Nano-crystalline. The molar ratios of the metal in the mixed oxides are close to the value in the starting solutions (synthesis molar ratio). The results demonstrate that the degrees of the precipitation of the metals are about 95%, and the mixed oxides are homogenous.

XRD patterns of Cu-Mg-Al hydrotalcite were given in figure 3. Peaks at 11.7, 23.6, 34.5, 39.7, 47.1, and 60.9°²² (JCPDS 35-0965). However, these peaks became broad and their intensity decreased with increasing the molar ratio of M²⁺ to M³⁺. Absence of other phases suggests that Cu²⁺ isomorphically replaced Mg²⁺ cations in the brucite-like layers, which can be related to the similar ionic radii of Cu²⁺ and Mg²⁺²⁴. A higher ordering of the lamellar layers can be clearly noticed with decreasing copper content, as indicated by both the increase in intensity and sharpness of (110) and (113) reflections. This effect was expected due to Jahn-Teller distortion at higher copper loadings, leading to the poor long range ordering²³. Based on the rhombohedral symmetry of hydrotalcites, the lattice parameters “a” and “c” were calculated. The parameter “a” is the same for all samples like 3.0, showing the isomorphous substitution of Mg by Cu cations in the brucite layers. There was a slight decrease of the parameter “c” with increasing copper content, related to a decrease in the interlayer distance, as observed²⁴. Calcination at 773-823 K, the characteristic lamellar structure disappears and XRD patterns show the presence of CuO tenorite (JCPDS 48-1548) and MgO periclase (JCPDS 45-946) phases. The average particle size was calculated as 20 nm by the Scherer equation. These results indicate that aluminum oxides are well dispersed in CuO–MgO matrix without segregation of a spinel-phase. CuAl₂O₄ spinel was formed from Cu–Mg–Al hydrotalcites only after calcination above 773-823K²⁵.

XRD pattern of calcined Nano hydrotalcite was given figure 4. Calcined hydrotalcite shows a peak at 43 and 63° are characteristic of hydrotalcite²⁶. All the hydrotalcite is calcined at 773-823K Under this temperature, Al³⁺ substitutes isomorphously to the Mg²⁺/Cu²⁺/ Zn²⁺ at the highest level, and M²⁺ coordinates with O²⁻ as most as possible. However, the basicity of coordination of M²⁺ with O²⁻ is higher than that of Al³⁺ with O²⁻^{16, 27}

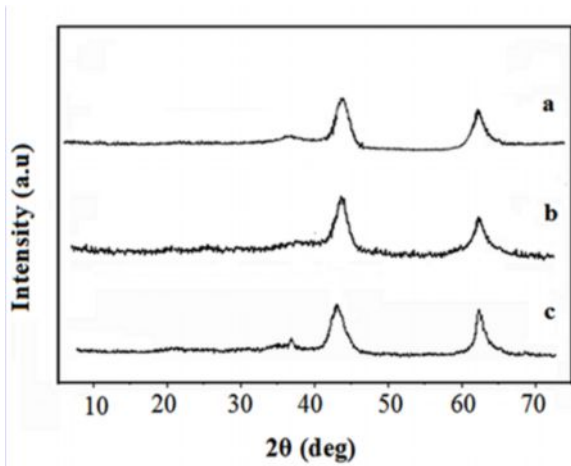


Figure 4: XRD pattern of calcined Nano hydrotalcite at 773-823 K (a). Zn-Mg -Al (b). Ni-Mg-Al (c). Cu-Mg-Al

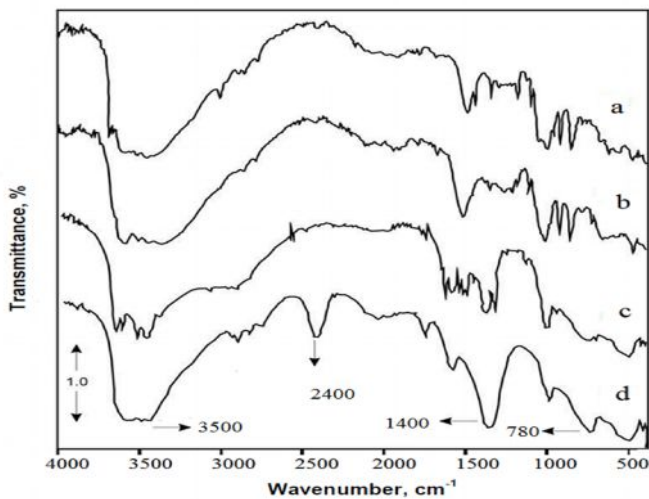


Figure 5: FT-IR spectra of (a). 2:2:1 (b). 2:3:1 (c). 3:3:1 (d). 3:5:1 molar ratio of Zn-Mg- Al Nano Hydrotalcite

FT-IR analysis

FT-IR spectroscopy of Zn-Mg-Al showed characteristic frequencies associated with the presence of intercalated anions. In all samples, a broad band at 3500 cm⁻¹ was observed (Figure 5) and represents the stretching vibrations of the OH groups of the inorganic and interlayer water. If the various metals in the hydrotalcites are distributed at random, in most cases, one hydroxyl group will be coordinated by at least two different metal cations²⁸. Another common frequency for LDH like materials is the presence of the bending vibrations of water molecules at 1600 cm⁻¹²⁹. Band at 1400 cm⁻¹ may indicate CO₃²⁻ are present in the interlayer of the hydrotalcite³⁰. The band located around 780 cm⁻¹ identified in the FTIR spectra may be due to the Al-O, Zn-Al-O, or Mg-Al-O band.

FT-IR pattern of Ni-Mg-Al was given in figure 6. In all samples, a broad band at 3500 cm^{-1} was observed and represents the stretching vibrations of the OH groups of the interlayer and water molecule. Frequency around 1381 cm^{-1} is due to the presence of nitrate in the interlayers while a band around 1362 cm^{-1} was noted for carbonate ion. Another common frequency at 1640 cm^{-1} is due to the bending vibrations of water molecules²⁹.

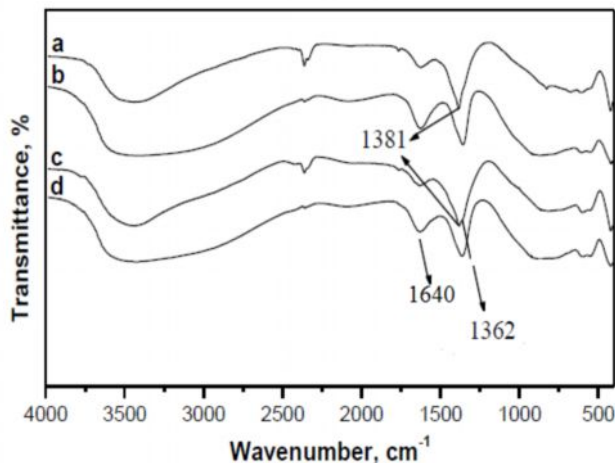


Figure 6: FT-IR spectra of (a). 2:2:1 (b). 2:3:1 (c). 3:3:1 (d). 3:5:1 molar ratio of Ni-Mg-Al

Nano Hydrotalcite

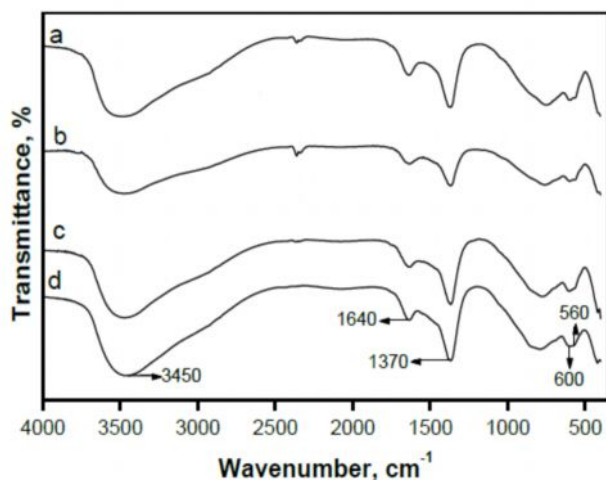


Figure 7: FT-IR spectra of (a). 2:2:1 (b). 2:3:1 (c). 3:3:1 (d). 3:5:1 molar ratio of Cu-Mg-Al Nano Hydrotalcite

FT-IR spectra of Cu-Mg-Al were given in figure 7. In all samples, a broad band at 3450 cm^{-1} was observed and represents the stretching vibrations of the OH groups of the interlayer and water molecule. Band at 1640 cm^{-1} is due to the bending vibrations of water molecules. Band around 1370 cm^{-1} is due to the presence of nitrate in the interlayers. The band located around 560 and 600 cm^{-1} identified which is due to the spectra of Al-O, Cu-Al-O, or Mg-Al-O bond.

BET surface area measurement

The BET surface area of calcined samples having different composition is given in table 1, 2 and 3. Thermal decomposition of hydrotalcite precursors led to the formation of high surface area. Also creation of large surface area is an important characteristic needed for catalysis. Surface areas of calcined hydrotalcite were

significantly higher than in uncalcined hydrotalcite samples³¹. The increase in surface area during calcination at 773-823 K can be attributed to the formation of mesopores due to expulsion of CO₂ and H₂O from the hydrotalcite precursors³². The higher basicity and higher surface area are found in 3:3:1 molar ratio of Zn-Mg-Al, 3:3:1 molar ratio of Cu-Mg-Al and 2:3:1 molar ratio of Ni-Mg-Al hydrotalcite. Divalent metal ion Zn²⁺/Cu²⁺/Ni²⁺ metal-support interaction in the Mg-O lattice that modifies the atomic and electronic structure of catalyst³³.

Table 1: Chemical composition analysis and physicochemical properties of Zn-Mg-Al Nano Hydrotalcite

Catalysts	Theoretical ratio of Zn-Mg-Al	Experimental ratio ^a Zn-Mg-Al	Unit cell parameters (Å)			BET surface area (m ² /g) ^b
			a	c	c'	
Zn-Mg-Al	2:2:1	1.96/1.89/1	3.042	22.73	7.31	166.4
	2:3:1	1.93/1.98/1	3.058	22.89	7.57	188.6
	3:3:1	3.02/2.98/1	3.063	22.95	7.72	220.8
	3:5:1	2.85/4.08/1	3.088	23.59	7.94	208.4

^a Experimental Zn-Mg-Al atomic ratios in the synthesized catalyst determined by EPMA.

^b BET surface area calcined at 773 -823 K/ overnight.

Table 2: Chemical composition analysis and physicochemical properties of Ni-Mg-Al Nano Hydrotalcite

Catalysts	Theoretical ratio of Cu-Mg-Al	Experimental ratio ^a Cu-Mg-Al	Unit cell parameters (Å)			BET surface area (m ² /g) ^b
			a	c	c'	
Cu-Mg-Al	2:2:1	1.82/1.84/1	3.075	22.72	7.48	157.8
	2:3:1	1.89/1.98/1	3.062	22.89	7.57	177.6
	3:3:1	3.12/2.82/1	3.062	22.82	7.68	192.5
	3:5:1	2.81/4.12/1	3.072	23.62	7.82	172.6

^a Experimental Ni-Mg-Al atomic ratios in the synthesized catalyst determined by EPMA.

^b BET surface area calcined at 773 -823 K/ overnight.

Table 3: Chemical composition analysis and physicochemical properties of Cu-Mg-Al Nano Hydrotalcite

Catalysts	Theoretical ratio of Ni-Mg-Al	Experimental ratio ^a Ni-Mg-Al	Unit cell parameters (Å)			BET surface area (m ² /g) ^b
			a	c	c'	
Ni-Mg-Al	2:2:1	1.86/1.81/1	3.057	22.85	7.51	169.7
	2:3:1	1.92/1.98/1	3.048	22.91	7.52	199.5
	3:3:1	3.20/2.81/1	3.071	22.93	7.63	181.4
	3:5:1	2.91/4.28/1	3.082	23.61	7.83	179.7

^a Experimental Cu-Mg-Al atomic ratios in the synthesized catalyst determined by EPMA.

^b BET surface area calcined at 773 -823 K/ overnight.

Transesterification of Ilupaoil (*Madhuca longifolia*)

A specified amount of catalyst and the required volume of methanol were added to the reaction mixture to Ilupa oil (*Madhuca longifolia*). The reactant mixture was then heated at various temperature ranges under

maximum agitation. This transesterification reaction could be mainly influenced by the following factors: amount of catalysts, reaction temperature, reaction time, methanol/oil molar ratio, and molar ratio of catalyst.

Amount of catalysts

The effect of catalyst amount on FAME yield was studied, when increasing the amount of catalyst, the slurry (mixture of catalyst and reactants) becomes too viscous possibly due to the rise of mixing problem of reactants, products, and solid catalyst and a demand of higher power consumption for adequate stirring. On the other hand, when the catalyst amount is not sufficient, the maximum conversion cannot be reached. Therefore, the optimum catalyst loading for the transesterification of the Ilupa oil (*Madhuca longifolia*) were found to be 7.5 g. We have already reported Zn-Mg-Al Nano catalysts with catalyst loading 7.5 g gives triglyceride conversion at 92.5 % for the transesterification of neem oil (*Azadirachta indica*)¹¹.

Effect of reaction time

The rate of transesterification reaction is strongly influenced by the reaction time. The conversion increased progressively with increasing reaction time and then reached a plateau value representative of a nearly equilibrium conversion. All catalysts gave a maximum conversion at 4 hour reaction time; after 4 hour reaction time yield was decreased probably due to reverse reaction (formation of triglycerides).

Effect of reaction Temperature

The effect of reaction temperature on the ester conversion was studied with the catalyst at various temperatures in figure 8. The transesterification proceeded slowly at 45°C; at lower temperatures, it resulted in a drop of the ester conversion because only a small amount of molecules was able to get over the required energy barrier. The optimum temperature for the preparation of the ester was found to be 65°C, which was near the boiling point of anhydrous methanol. The conversion fall to about 60% in the temperature range of 75°C, probably because the molar ratio of methanol to oil decreased when methanol reactant volatilized into the gas phase above 65°C, the boiling point of pure methanol. The ester conversion increased up to 92.5%, 86.5 and 67.4 % for Zn-Mg-Al, Ni-Mg-Al and Cu-Mg-Al Nano hydrotalcite respectively at temperature 65°C.

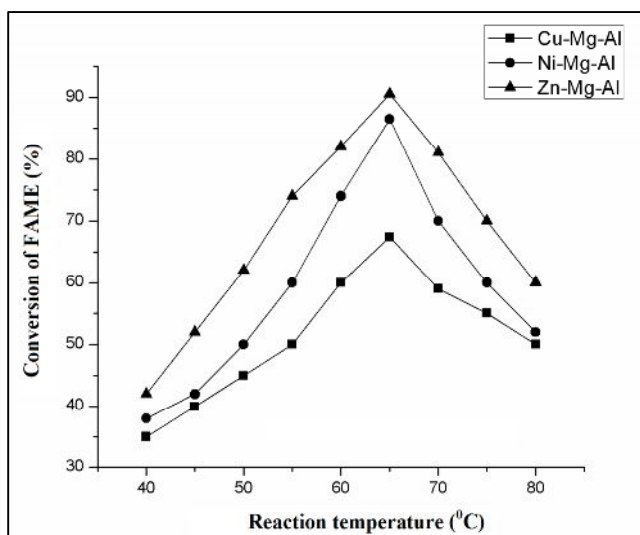


Figure 8: Effect of reaction temperature on conversion of FAME (%)

Effect of Molar Ratio and Catalytic Studies

The effect of molar ratio and the catalytic activity studied at 65°C were illustrated in figure 9, which indicates that the catalytic activity was improved with the increase in Zn and Mg content in Zn-Mg-Al molar ratio at 3:3:1; but the increase in the Mg content in Zn-Mg-Al molar ratio of 3:5:1, the catalytic activity dropped. Catalytic activity was improved in 2:3:1 molar ratio of Ni-Mg-Al but the increase in Ni content in Ni-Mg-Al molar ratio of 3:3:1 and 3:5:1, the catalytic activity dropped. In the case of Cu-Mg-Al maximum catalytic activity obtained at 3:3:1 molar ratio, but the catalytic activity dropped at 3:5:1. The catalytic activity decreased in samples due to the formation of surface amorphous Al-O structure that partially covered Mg-O pairs and decreased the concentration surface O^{2-} . The increased catalytic activity of the tertiary oxide system was due to the modification of the electronic properties between the oxides³⁴.

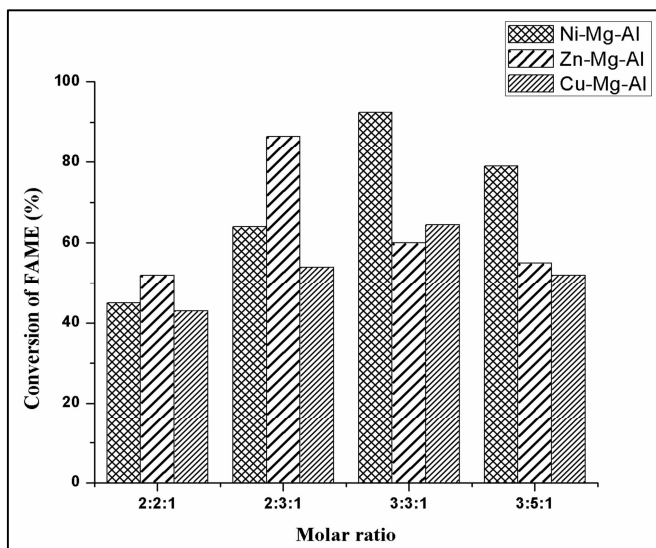


Figure 9: Effect of Molar ratio on Conversion of FAME (%) at 65 °C

Table 4: Effect of Molar ratio on product selectivity and conversion

Catalyst	Catalyst molar ratio	Conversion Wt (%)	Product Selectivity Wt (%)	
			FAME	Glycerol
Zn-Mg-Al	2:2:1	32	43.49	23.51
	2:3:1	43	65.12	19.88
	3:3:1	56	92.5	10.02
	3:5:1	49	88.3	6.35
Ni-Mg-Al	2:2:1	45	52.4	37.42
	2:3:1	51	86.5	12.73
	3:3:1	40	60.2	20.22
	3:5:1	44	55.42	32.45
Cu-Mg-Al	2:2:1	57	43.47	27.23
	2:3:1	43	54.23	30.74
	3:3:1	41	64.42	18.27
	3:5:1	44	52.34	31.27

Table 4 reveals various molar ratios of hydrotalcite with product selectivity. The high activity of hydrotalcite is due to the surface site of low (OH^- group), medium (Mg-O pairs), and strong (O^{2-} anions) basicity²⁸. The catalytic activity of the catalyst is also monitored through the percentage extent of formation of fatty acid methyl ester and glycerol conversion. Zn-Mg-Al Nano hydrotalcite with molar ratio 3:3:1 gave conversion rate of 92.5%, Ni-Mg-Al Nano hydrotalcite with molar ratio 2:3:1 the highest conversion rate of 86.5% and Cu-Mg-Al Nano hydrotalcite with molar ratio 3:3:1 gave conversion rate of 67.4% was attained. The higher catalytic activity of Zn-Mg-Al, Ni-Mg-Al and Cu-Mg-Al indicates the higher acidity of this catalyst which can be attributed to the dissolution of more amount of Al^{3+} in the M (II) -O lattice introducing Lewis

acidity. Also the Zn^{2+} / Ni^{2+} / Cu^{2+} ions in Mg^{2+} lattice, the acidic centers submerged in the basic matrix, may be resulting in concomitant acidic-basic centers and more in the presence of considerable amount of Lewis acidity in these compounds [29].

In the case of Ni-Mg-Al with 2:3:1 gave maximum activity which is due the higher surface area than the other molar ratio, Ni^{2+} ions in Mg^{2+} lattice, acidic centers submerged in the basic matrix and also presence of more amount Lewis acid sites in these compounds. The amount of acidic sites is dropped by increasing Ni ion in Mg-Al matrix. All other ratios except 2:3:1 lower number of basicity was found; this indicated that medium basic strength is less influencing in transesterification rate.

Similarly Cu-Mg-Al with 3:3:1 gave maximum catalytic activity probably due to the acidic centers submerged in the basic matrix, higher surface area and also highest number of basicity. According to literature study, the main factor to influence transesterification activity is the alkalinity and the type of basic strength of the catalysts^{34, 35}. The author previously reported that the Mg^{2+}/Al^{3+} hydrotalcites at ratio 3.0 showed higher acidity of this catalyst which can be attributed to the dissolution of more amount of Al^{3+} in the M (II) -O lattice introducing Lewis acidity and also contain high density of Al-O pairs; lower and medium strength basic sites $Al^{3+}-O^{2-}$ pairs do not contribute much to the surface basicity. In contrast, both M (II) and M (III) cations provide Lewis acidic sites²⁸. The conversion and the viscosity of produced ester depended on the molar ratio of methanol to vegetable oil, which was one of the most important variables. The high yield of biodiesel was achieved when the methanol oil molar ratio was 10:1. Increase in the methanol loading amount, the viscosity was slightly decreased and could ensure complete reaction. Excessive methanol had no significant effect on the yield¹². From the experimental results, it can be concluded that the optimum conditions for the transesterification of Ilupa oil (*Madhuca longifolia*) catalyzed by Zn-Mg-Al, Ni-Mg-Al and Cu-Mg-Al Nano hydrotalcite at temperature 65 °C, reaction time 4 hours, catalyst loading 7.5 g and methanol to oil molar ratio was 10:1.

SEM images of Hydrotalcite had a relatively uniform hexagonal platelet-like structure, but partly destroyed at the calcined temperature of 773 K. The platelets were formed by agglomeration with numerous fine nanoparticles. SEM image of Zn-Mg-Al shows thin platelets with lamellar morphology (Figure 10), Ni-Mg-Al shows hexagonal platelet with coral morphology (Figure 11) and Cu-Mg-Al shows hexagonal thin platelets with crystal morphology (Figure 12). The formation of Nano-crystalline hydrotalcite derived mixed oxides could be due to the divalent ion (Zn^{2+} , Ni^{2+} , Cu^{2+}) influence in the nucleation and crystal growth process during co-precipitation.

Biodiesel produced from the Ilupa oil (*Madhuca longifolia*) was analyzed by gas chromatography. It conforms biodiesel compositions like palmitic acid (C16:0), palmitoleic acid (C16:1), stearic acid (C18:0), oleic acid (C18:1), linoleic acid (C18:2), and linolenic acid (C18:3). The identified composition is compared with standard compounds. From the analysis data confirmed, the product is the biodiesel phase of the methyl esters.

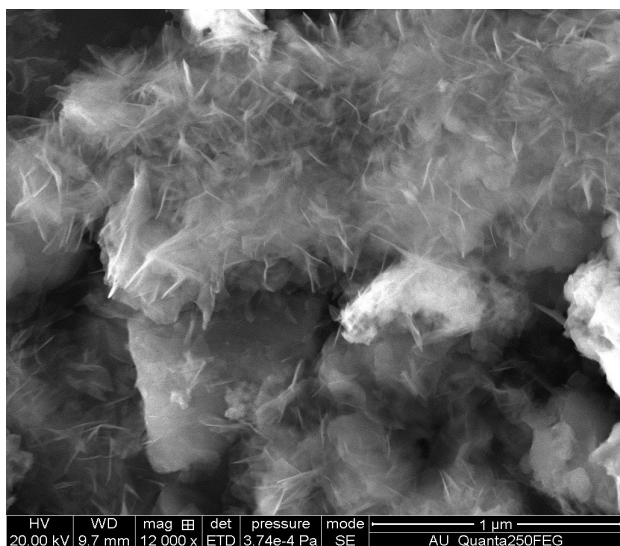


Figure 10: SEM image of Zn-Mg-Al Nano hydrotalcite

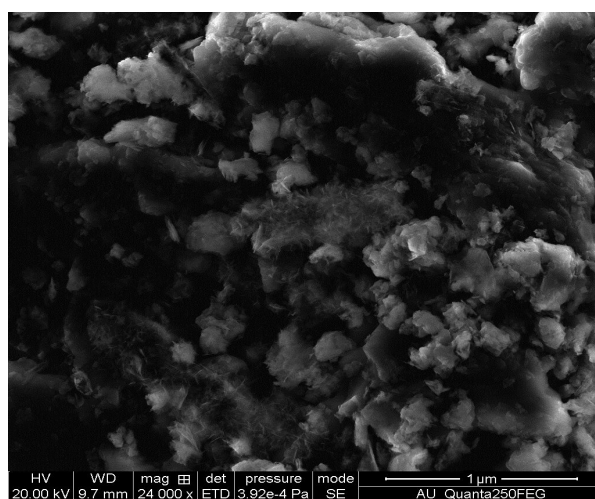
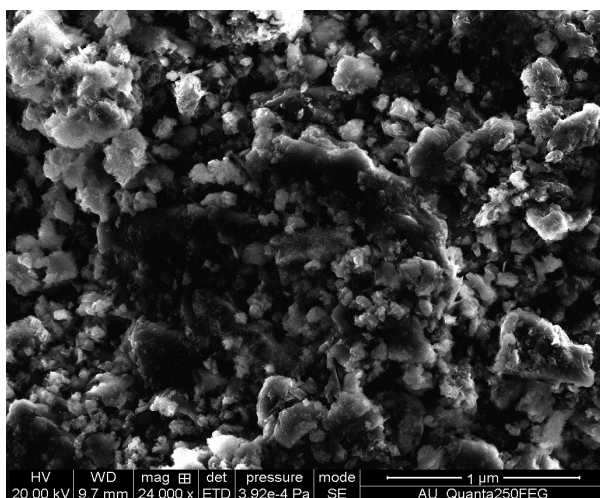


Figure 11: SEM image of Ni-Mg-Al Nano hydrotalcite

Figure 12: SEM image of Cu-Mg-Al Nano hydrotalcite

Conclusions

The present work deals with the transesterification of Ilupa oil (*Madhucal longifolia*) was studied in a heterogeneous system using calcined Zn-Mg-Al, Ni-Mg-Al and Cu-Mg-Al Nano hydrotalcites as solid base catalysts. The effects on biodiesel production of the methanol/oil molar ratio, reaction temperature, reaction time and catalysts amount were studied. The optimum reaction conditions were found to be at temperature 65 °C, reaction time 4 hours, catalyst loading 7.5 g and methanol to oil molar ratio was 10:1. Zn-Mg-Al Nano hydrotalcite with molar ratio 3:3:1 exhibited maximum catalytic activity for transesterification reaction with methanol and gave conversion rate of 92.5%, Ni-Mg-Al Nano hydrotalcite with molar ratio 2:3:1 the highest conversion rate of 86.5% and Cu-Mg-Al Nano hydrotalcite with molar ratio 3:3:1 conversion rate of 67.4% was achieved. It could be concluded that the Calcined Nano hydrotalcite have numerous advantages for transesterification of vegetable oil such as high catalytic activity, easy separation, recycling of the catalyst, nontoxic and inexpensive catalysts.

References:

1. Ma F and Hanna M. A, "Biodiesel production: a review," *Biore. Tech.*, 1999, 70, 1–15.
2. Ramadhas A S, Jayaraj S, and Muraleedharan C, "Biodiesel production from high FFA rubber seed oil", *Fuel*, 2005, 84, 335-340.
3. S.K. Karmee and A. Chadha, "Preparation of biodiesel from crude oil of *Pongamia pinnata*", *Biore. Tech.*, 2005, 96, 1425-1429.
4. Brito A, Borges M. E, Garin M, and Hernandez A, "Biodiesel Production from Waste Oil Using Mg-Al Layered Double Hydroxide Catalysts," *Energy & Fuels*, 2009, 23, 2952–2958.
5. Cavani F, Trifiro F, and Vaccari A, "Hydrotalcite-type anionic clays: preparation, properties and applications," *Catal. Today*, 1991, 11, 173–301.
6. Guida A, Hassane L M, Tichit D, Figueras F and Geneste P, "Hydrotalcites as base catalysts. Kinetics of Claisen-Schmidt condensation, intramolecular condensation of acetylacetone and synthesis of chalcone" *Appl. Catal.:A*, 1997, 164, 251-264.
7. Rao K K, Gravelle M, Sanchez-Valente J and Figueras F, "Activation of Mg-Al hydrotalcite catalyst for aldol condensation reactions", *J.Catal.*, 1998, 173, 115-121.
8. Tichit D, Benanni M N, Figueras F, Tessier R and Kervennal J, "Aldol condensation of acetone over layered double hydroxides of the meixnerite type," *Appl. Clay Sci.*, 1998, 13, 401-410.
9. Roelofs J C A A, Lensveld D J, A. Van Dillen J and De Jong K P, "On the Structure of Activated Hydrotalcites as Solid Base Catalysts for Liquid-Phase Aldol Condensation", *J. catal.*, 2001, 203, 184-191.
10. Prinetto F, Tichit D, Teissier R and Coq B, "Mg-and Ni-containing layered double hydroxides as soda substitutes in the aldol condensation of acetone", *Catal.Today*, 2000, 55, 103-116.
11. Manivannan R and Karthikeyan C, "Synthesis of biodiesel from neem oil using Mg-Al nano hydrotalcite," *Adv. Mater. Res.*, 2013, 678, 268–272.

12. Karthikeyan C and Manivannan R, "Environmentally Benign Neem Biodiesel Synthesis Using Nano-Zn-Mg-Al Hydrotalcite as Solid Base Catalysts," *J. Catal.*, 2014,14,1-6.
13. Climent M J, Corma A, Iborra S, Epping K, and Velty A, "Increasing the basicity and catalytic activity of hydrotalcites by different synthesis procedures," *J. Catal.*, 2004, 225, 316–326.
14. Parida K and Das J, "Mg/Al hydrotalcites: preparation, characterisation and ketonisation of acetic acid," *J. Mol. Catal. A: Chem.*, 2000, 151, 185–192.
15. Tichit D, Lhouty M H, and Guida A, "Textural properties and catalytic activity of hydrotalcites," *J. Catal.*, 1995, 151, 50–59.
16. Di Cosimo J I, Díez J V, Xu M, Iglesia E, and Apesteguía C.R, "Structure and surface and catalytic properties of MgAl basic oxides," *J. Catal.*, 1998, 178, 499–510.
17. Constantino V R L and Pinnavaia T J, "Basic properties of $Mg^{2+}_{1-x} Al^{3+}$ layered double hydroxide intercalated by carbonate, hydroxide, chloride and sulfate anions," *In. Chem.*, 1995, 34, 883–892.
18. Miyata S and Okada A, "Synthesis of hydrotalcite-like compounds and their physico-chemical properties—the systems $Mg^{2+}-Al^{3+}-SO_4^{2-}$ and $Mg^{2+}-Al^{3+}-CrO_4^{2-}$," *Clay. Miner.*, 1977, 25, 14–18.
19. Birks L S and Friedman H, "Particle size determination from x-ray line broadening," *J. Appl. Phys.*, 1946, 17, 687–691.
20. Tichit D, Medina F, Coq B, and Dutartre R, "Activation under Oxidizing and Reducing Atmospheres of Ni-containing Layered Double Hydroxides", *Appl. Catal.*, 1997, 159, 241–258.
21. Shishido T, Sukenobu M, Morioka H, Furukawa R, Shirahase H and Takehira K, "CO₂ reforming of CH₄ over Ni/Mg-Al oxide catalysts prepared by solid phase crystallization method from Mg-Al hydrotalcite-like precursors", *Catal. Lett.*, 2001, 73, 21–26.
22. Ferreira K A, Ribeiro N F P, Souza M M V M, Schmal M, Structural Transformation of Cu-Mg-Al Mixed Oxide Catalysts Derived from Hydrotalcites During Shift Reaction, *Catal. Lett.*, 2009, 132, 58-63.
23. Kannan S, Dubey A, and Knozinger H, "Synthesis and characterization of Cu-Mg-Al ternary hydrotalcites as catalyst for hydroxylation of phenol", *J. Catal.* 2005, 231, 381-392.
24. Chmielarz L, Kustrowski P, Rafalska-Łasocha A, Majda D, and Dziembaj R, "Catalytic activity of Co-Mg-Al, Cu-Mg-Al and Cu-Co-Mg-Al mixed oxides derived from hydrotalcites in SCR of NO with ammonia", *Appl. Catal. B: Env.*, 2002, 35, 195-21.
25. Kovanda F, Jiratova K, Rymes J and Kolousek D "Characterization of activated Cu/Mg/Al hydrotalcites and their catalytic activity in toluene combustion, *Appl. Cl. Sci.*, 2001, 18, 71-80.
26. Mustrowski P, Chmielarz L, Bozek E, Sawalha M and Roessner F, "On Synthesis of Nano synthesized material," *Mat. Res. Bul.* 2004, 39, 263-294.
27. Kottapalli K R, Monique G, Jaime S V, and Francois F, "Activation of Mg-Al Hydrotalcite Catalysts for Aldol Condensation Reactions", *J. Catal.*, 1998, 173, 115-121.
28. Manivannan R and Pandurangan A, "Formation of ethyl benzene and styrene by side chain methylation of toluene over calcined LDHs," *Appl. Cl. Sci.*, 2009, 44, 137–143.
29. Manivannan R and Pandurangan A, "Side chain ethylation of toluene with ethanol over hydrotalcite-like compounds," *Kin. and Catal.*, 2010, 51, 56–62.
30. Davila V, Lima E, Bulbulian S, and Bosch P, "Mixed Mg (Al) O oxides synthesized by the combustion method and their recrystallization to hydrotalcites," *Micro. Meso. Mat.*, 2008, 107, 240–246.
31. Kanazaki E, "Intercalation of naphthalene-2,6-disulfonate between layers of Mg and Al double hydroxide: preparation, powder X-ray diffraction, fourier transform infrared spectra and X-ray photoelectron spectra," *Mat. Res. Bul.*, 1999, 34, 1435–1440.
32. Corma A, Hamid S B A, Iborra S, and Velty A, "Lewis and Bronsted basic active sites on solid catalysts and their role in the synthesis of monoglycerides," *J. Catal.*, 2005, 234, 340–347.
33. Kazansky V B, Borovkov V Y, and Derouane E G, "Diffuse reflectance IR-spectroscopy evidence of the unusual properties of platinum in Pt/Mg(Al)O catalysts for the selective aromatization of n-alkanes," *Catal. Lett.*, 1993, 19, 327–331.
34. V. B. Kazansky, V. Y. Borovkov, and E. G. Derouane, "Diffuse reflectance IR-spectroscopy evidence of the unusual properties of platinum in Pt/Mg(Al)O catalysts for the selective aromatization of n-alkanes," *Catalysis Letters*, vol. 19, no. 4, pp. 327–331, 1993.
35. X. Deng, Z. Fang, Y. H. Liu, and C. L. Yu, "Production of biodiesel from *Jatropha* oil catalyzed by Nano sized solid basic catalyst," *Energy*, vol. 36, no. 2, pp. 777–784, 2011.
